Available online at www.sciencedirect.com
SCIENCE DIRECT®
Atmospheric Environment 39 (2005) 315–327
ATMOSPHERIC ENVIRONMENT
www.elsevier.com/locate/atmosenv

Reactive nitrogen oxides in the southeast United States national parks: source identification, origin, and process budget

Daniel Quansong Tong[a,*], Daiwen Kang[a,1], Viney P. Aneja[a], John D. Ray[b]

[a]*Department of Marine, Earth and Atmospheric Sciences, North Carolina State University, Raleigh, NC 27695-8208, USA*
[b]*Air Resources Division, National Park Service, Denver, CO 80225-0287, USA*

Received 23 November 2003; received in revised form 27 August 2004; accepted 6 September 2004

Abstract

We present in this study both measurement-based and modeling analyses for elucidation of source attribution, influence areas, and process budget of reactive nitrogen oxides at two rural southeast United States sites (Great Smoky Mountains national park (GRSM) and Mammoth Cave national park (MACA)). Availability of nitrogen oxides is considered as the limiting factor to ozone production in these areas and the relative source contribution of reactive nitrogen oxides from point or mobile sources is important in understanding why these areas have high ozone. Using two independent observation-based techniques, multiple linear regression analysis and emission inventory analysis, we demonstrate that point sources contribute a minimum of 23% of total NO_y at GRSM and 27% at MACA. The influence areas for these two sites, or origins of nitrogen oxides, are investigated using trajectory-cluster analysis. The result shows that air masses from the West and Southwest sweep over GRSM most frequently, while pollutants transported from the eastern half (i.e., East, Northeast, and Southeast) have limited influence ($<10\%$ out of all air masses) on air quality at GRSM. The processes responsible for formation and removal of reactive nitrogen oxides are investigated using a comprehensive 3-D air quality model (Multiscale Air Quality SImulation Platform (MAQSIP)). The NO_y contribution associated with chemical transformations to NO_z and O_3, based on process budget analysis, is as follows: 32% and 84% for NO_z, and 26% and 80% for O_3 at GRSM and MACA, respectively. The similarity between NO_z and O_3 process budgets suggests a close association between nitrogen oxides and effective O_3 production at these rural locations.

Keywords: Nitrogen oxides; Ozone; Atmospheric chemistry; Budget analysis

1. Introduction

Ambient O_3 concentrations found in the lower troposphere remain a major air pollution problem in urban areas of the United States (National Research Council (NRC), 1991; Lippmann, 1992). Despite the fact that significant controls on O_3 precursors have been implemented, rural areas in the southeast United States continue to suffer from periodic high O_3 episodes during summertime (NRC, 1991; Aneja et al., 1991; Chameides et al., 1998; US Environmental Protection Agency (EPA), 2001). Several eastern US national parks observed high O_3 concentrations (Table A-20,

*Corresponding author. Tel.: +1 609 258 4832.
E-mail address: quansong@princeton.edu (D.Q. Tong).
[1]Now at Atmospheric Modeling Division, NERL/US EPA, Research Triangle Park, NC 27711.

1352-2310/$ - see front matter © 2004 Elsevier Ltd. All rights reserved.
doi:10.1016/j.atmosenv.2004.09.035

EPA, 2001). Among them, the Great Smoky Mountains National Park has experienced the most rapid increase in the frequency of exceedance days (days when any 8-h average O_3 concentration exceeding 85 ppbv) during the last decade. The increasing trend in the number of O_3 exceedances is unexpected since the park is located in a rural area and is a mandatory Class I area under the Clean Air Act Amendments of 1990. In 1997, the US EPA proposed a new National Ambient Air Quality Standard (NAAQS) for O_3 and other crucial pollutants. Previous analysis of measurements from the former Aerometric Information Retrieval System (AIRS) monitoring network showed that the new NAAQS would almost triple the number of nonattainment counties in the United States (EPA, 1999).

A previous modeling study (Kang et al., 2003) indicates that there are differences in O_3 production potential and VOC reactivity among the three National Park Service (NPS) enhanced-monitoring sites in the Shenandoah (SHEN), Mammoth Cave (MACA), and Great Smoky Mountains (GRSM) national parks. Kang et al. (2001) reported from measurements that more than 90% of the chemical reactivity of VOCs at GRSM is from isoprene. Budget analysis from a modeling study indicates that 67–95% of the VOCs can be attributed to local emissions (Kang et al., 2003). Thus, understanding the contribution of nitrogen oxides to O_3 formation during transport and local photochemistry is essential to predicting what effect planned reductions in NO_x emissions from large point sources might have on observed O_3 concentrations at these southeast national parks.

Ambient data—including intermittent hydrocarbon samples and continuous measurements of ozone (O_3), total reactive oxides of nitrogen (NO_y), nitric oxide (NO), sulfur dioxide (SO_2), and carbon monoxide (CO)—were collected at two southeast national parks. The observation-based air chemistry and O_3 nonattainment have been discussed elsewhere (Tong et al., submitted manuscript, 2004). This study deals with data analysis and modeling study based on measurements collected from 1995 to 1998. These results, together with the air chemistry observations (Tong et al., submitted manuscript, 2004) and previous study of nonmethane hydrocarbons (Kang et al., 2001, 2003), are expected to advance our knowledge of the controlling factors affecting O_3 exceedances at the southeast national parks and more extensive rural areas with similar environmental settings. Our specific interests in this study are the following: (1) to quantify the relative importance of point sources and mobile sources to total nitrogen oxides emissions; (2) to identify the origin of air masses associated with high levels of nitrogen oxides and O_3; and (3) to investigate contributions of individual processes to the budget of production and removal of nitrogen oxides in the southeast national parks.

2. Measurements and methodology

2.1. Measurements

O_3, NO_y, NO, SO_2, CO, and other meteorological parameters were measured at two enhanced monitoring sites in the southeast United States (TVA, 1995; Olszyna et al., 1998). The Great Smoky Mountains (GRSM) site (35°41′48″N, 83°36′35″W), at 1243 m above sea level, is located at the summit of Cove Mountain in the Great Smoky Mountains national park in Sevier County, Tennessee. The Mammoth Cave (MACA) site (37°13′04″N, 86°04′25″W), at 230 m above sea level, is located in the Mammoth Cave national park approximately 5 miles from Cave City, Kentucky, in a clearing about 30 m from the surrounding forest area. Ambient air samples for O_3, SO_2, and CO were collected through a Teflon tube equipped with 5-μm Teflon particulate filters. Samples of O_3, SO_2, and CO were analyzed using O_3 Model 49, SO_2 Model 43S, and CO Model 48S monitors from Thermo Environmental Instruments, Incorporated (TEII). Air samples for NO and NO_y were each collected separately through $\frac{1}{4}''$ OD Teflon sampling lines. NO and NO_y were analyzed using a TEII Model 42S with an external Mo converter operated in a time-sharing mode to measure the two trace gases separately. Gases used for calibration and daily quality assurance/quality control (QA/QC) activities were EPA Protocol SO_2, CO, NO, and NO_2 gas cylinders provided by Scott-Marin. For routine QA/QC activities, a Campbell CR10 data logger was configured to automatically control gas influx, sampling switches, gas addition, and gas substitution. A TEII 111 Zero Air generating system and a TEII 146 Dynamic Gas Calibrator were also used. A CO catalytic reactor in the TEII Model 111 provided CO-free ambient air for zero checks and correction of instrument drift.

Measurement operations followed the QA/QC procedures established for the Level II ground-based air monitoring stations that participated in the SOS/Nashville 1995 Intensive (TVA, 1995). The procedure consists of zero, span, and precision checks using gas-substitution/gas-addition techniques that determined matrix effects in the sampling system. Addition of NO at the midday median NO_y concentration was conducted to both NO_y and NO sampling lines three times a day. Measurements for O_3 were conducted according to SLAMS protocol, modified to operate the O_3 instrument in the range from 0 to 200 ppbv. More detailed information on instruments, experimental techniques, and data QA/QC procedures can be found from Olszyna et al. (1998) and in the TVA AQ/QC manual.

2.2. Emission source strength: point vs. mobile sources

According to the US EPA, more than 90% of the anthropogenic NO_x ($NO_x = NO + NO_2$) emissions in the United States are from either mobile sources or point sources (EPA, 1997). Mobile sources emit high levels of CO but relatively low levels of SO_2; for point sources, the reverse is true. Therefore, NO_x emissions may correlate well with either SO_2 or CO, leaving relatively little NO_x unaccounted for (Stehr et al., 2000). In actual calculations, NO_x is replaced by NO_y, since some fraction of the pollutants is oxidized before arriving at the receptor site.

Relative emission-source strength can be quantified at a receptor site using observed pollutant data and the techniques of regression analysis and emission-inventory analysis. Emission-inventory analysis uses the molar ratios of NO_x to CO and NO_x to SO_2 reported by EPA emission inventories (1997). Regression analysis obtains these ratios by fitting a multivariant regression model to measured data. Both techniques use measured CO and SO_2 concentrations as input to estimate the relative contributions from point and mobile sources to total reactive nitrogen oxides.

2.2.1. Regression analysis

NO_y is taken as the response variable in a multiple-linear regression analysis and the combination of CO and SO_2 as factors. The mathematical expression of the fitted model is

$$[NO_y] = \alpha[SO_2] + \beta[CO] + \delta, \quad (1)$$

where α and β are the linear coefficients between $[NO_y]$ and $[SO_2]$ and [CO], respectively, and δ is the intercept. After α and β are parameterized, the model can be used to quantify relative contributions from mobile and point sources by plugging in measured CO and SO_2 concentrations.

Measurement data is divided into different categories to examine potential influences of seasonality and diurnal cycles on the valuation. The entire data set is divided into four groups based on seasonality—spring (March, April, and May), summer, fall, and winter—to explore the influence of seasonal variations. Each group is further divided into two subsets—daytime (1000–1500 EST, corresponding to the period of maximum photochemical activity) and nighttime (2300–0500 EST)—to examine day/night differences. After the models are fitted to each group, studentized residuals are used to remove outliers from each data set. Observations with an absolute studentized residual >2 were removed. To validate the assumptions of the linear regression model during each time period, the Durbin–Watson test was used to test the first-order autocorrelation. A Q–Q plot was employed to test the normality of the predicted residuals which suggest a normal distribution of residuals. The coefficients, α, β, and δ in Eq. (1) are determined using validated measurements from MACA and GRSM. Tables 1 and 2 present results of multiple-linear regression analysis for each season at GRSM and MACA. The ratios of $[NO_x]$ to $[SO_2]$ are 0.49 at GRSM, and 0.64 at MACA for all seasons. These values are in good agreement with the nationwide average emission inventory ratio of $[NO_x]/[SO_2]$ (0.64, EPA, 1997). They also stand within the estimated range of northeast study by Stehr et al. (2000), who reported a ratio of 0.75–0.88 for September–December at the high-elevation Shenandoah National Park, GA (1100 m above sea level), and

Table 1
Regression analysis on the dataset measured in the Great Smoky Mountain (GRSM) National Park, TN, for 1995–1998

Season	Time	Coeff. of $[SO_2]$	Coeff of [CO]	R^2	Intercept	Mean $[NO_y]$
Spring	All data	0.51±0.01	0.018±0.001	0.51	0.43±0.19	5.14
	Midday	0.71±0.04	0.015±0.021	0.54	0.65±0.43	5.01
	Midnight	0.50±0.02	0.020±0.002	0.61	−0.02±0.33	5.18
Summer	All data	0.30±0.01	0.015±0.001	0.57	0.13±0.12	3.55
	Midday	0.28±0.02	0.013±0.001	0.63	0.47±0.25	3.56
	Midnight	0.22±0.01	0.018±0.001	0.52	−0.17±0.21	3.47
Fall	All data	0.41±0.01	0.027±0.001	0.54	−1.32±0.15	3.91
	Midday	0.45±0.05	0.026±0.003	0.42	−1.26±0.43	4.26
	Midnight	0.43±0.03	0.023±0.001	0.57	−0.86±0.21	3.57
Winter	All data	0.68±0.04	0.013±0.002	0.37	1.2±0.33	4.91
	Midday	0.57±0.06	0.033±0.005	0.59	−2.49±0.87	4.72
	Midnight	0.91±0.09	0.006±0.004	0.28	2.53±0.55	5.21
Total	All data	0.49±0.01	0.019±0.001	0.44	−0.06±0.10	4.31
	Midday	0.49±0.02	0.021±0.001	0.46	−0.62±0.25	4.37
	Midnight	0.50±0.02	0.015±0.001	0.37	0.67±0.18	4.23

Table 2
Regression analysis on the dataset measured in the Mammoth Cave (MACA) national park, KY, for 1995–1998

Season	Time	Coeff. of [SO_2]	Coeff of [CO]	R^2	Interception	Mean [NO_y]
Spring	All data	0.56±0.01	0.034±0.001	0.37	−2.57±0.23	5.98
	Midday	0.74±0.02	0.023±0.002	0.55	−0.66±0.44	6.28
	Midnight	0.33±0.04	0.038±0.002	0.26	−3.28±0.41	5.45
Summer	All data	0.61±0.02	0.025±0.001	0.21	−0.79±0.24	5.00
	Midday	0.69±0.02	0.011±0.001	0.61	1.20±0.26	4.83
	Midnight	0.85±0.09	0.031±0.003	0.13	−1.93±0.57	5.13
Fall	All data	0.71±0.02	0.049±0.002	0.40	−4.35±0.30	6.97
	Midday	0.76±0.03	0.037±0.003	0.56	−2.51±0.44	6.71
	Midnight	0.71±0.04	0.051±0.003	0.35	−4.88±0.57	6.69
Winter	All data	0.57±0.01	0.061±0.001	0.61	−7.58±0.28	9.20
	Midday	0.62±0.03	0.067±0.003	0.69	−8.69±0.57	9.71
	Midnight	0.48±0.03	0.052±0.002	0.45	−5.40±0.51	8.77
Total	All data	0.64±0.01	0.041±0.001	0.44	−3.71±0.13	6.62
	Midday	0.74±0.01	0.037±0.001	0.62	−3.14±0.22	6.70
	Midnight	0.57±0.02	0.041±0.001	0.32	−3.55±0.25	6.36

lower ratios for two low-elevation sites (0.36–0.41 at Arendtsville, PA for June–September, and 0.18–0.48 at the Wye site for September–December). Tables 1 and 2 also reveal that [NO_x]/[SO_2] day/night differences are most significant in winter at both low and high elevations.

The ratios of [NO_x] to [CO] are 0.019 at GRSM and 0.041 at MACA, significantly lower than the nationwide value (0.084 EPA, 1997), as well as those reported by earlier studies (0.041–0.091, Stehr et al., 2000; 0.069, Goldan et al., 1995; 0.075±0.027, Buhr et al., 1992; 0.12, National Acid Precipitation Assessment Program (NAPAP), Saeger et al., 1989).

2.2.2. *Emission-inventory analysis*

Emission-inventory analysis has been used in earlier work (e.g., Parrish et al., 1991; Goldan et al., 1995; Stehr et al., 2000) to examine relationships between NO_y, CO, and SO_2. Briefly, the ratio (indicated by x) of NO_y from point sources ($NO_y|_p$) to mobile sources ($NO_y|_m$) can be obtained from the division of two factors:

$$x = \frac{NO_y|p}{NO_y|m} = \frac{NSRp}{NCRm}\left(\frac{\mu^*[SO_2]}{[CO]-[CO]_{bg}}\right), \quad (2)$$

where NSR_p and NCR_m represent the molar ratios of [NO_y] to [SO_2] from point sources and NO_y to CO from mobile sources, respectively. [SO_2] and [CO] are concentrations of SO_2 and CO measured at a receptor site; $[CO]_{bg}$ is background CO concentration that is independent of local processes. An adjusting parameter, μ, is introduced to account for the fraction of SO_2 that has been oxidized into sulfate before arriving at the receptor site. Therefore,

$$\text{fraction of } NO_y \text{ attributed to mobile sources} = 1/(1+x), \quad (3a)$$

$$\text{fraction of } NO_y \text{ attributed to point sources} = x/(1+x). \quad (3b)$$

The ratio of NO_y to SO_2 (i.e., $NSR|_p$ in Eq. (2)) for point sources and the ratio of NO_y to CO (i.e., $NCR|_m$ in Eq. (2)) for mobile sources are derived from anthropogenic state-level emission data (EPA, 1997). Emission data of 17 states are used to calculate the ratios for GRSM, and another 29 states for MACA. The extent of these sets of states was determined by back trajectory analysis described in the following section. Values of $NSR|_p$ and $NCR|_m$ are 1.70 and 0.19 for GRSM, and 2.09 and 0.20 for MACA, respectively. These ratios are approximately twice as high as those obtained by Stehr et al. (2000), which are mostly derived from emission data of the northeast states.

Theoretically, the CO background concentration, $(CO)_{bg}$, can be obtained from dividing the intercept by negative CO coefficient (-β as above) in Eq. (1) in regression analysis, since the value of the zero-[NO_y] intercept is believed to be mostly governed by CO background concentration (Stehr et al., 2000). The results of CO background concentration thereby calculated were found to deviate greatly from the expected range (Parrish et al., 1991; Doddridge et al., 1992; Warneck, 2000; Li et al., 2004). This deviation reflects both statistical uncertainties in regression analysis and

combined influences of SO_2 and NO_y emissions. Instead, Parrish et al. (1991) and Doddridge et al. (1992) express the ratio of CO to NO_y as

$$[CO] = \rho[NO_y] + [CO]_{bg}, \quad (4)$$

where ρ is the molar ratio $[CO]/[NO_y]$. The coefficient ρ may be different from the ratio $[CO]/[NO_y]$ (i.e., $1/\beta$ in Eq. (1)) in the multiple linear regression analysis since the other factor, $[SO_2]$, is excluded in this fitting model. The calculated CO background concentrations for spring, summer, fall, and winter are 183 ± 1, 179 ± 1, 168 ± 1, and 175 ± 1 at MACA, and 155 ± 2, 134 ± 2, 112 ± 2, and 138 ± 2 at GRSM, respectively. These results at GRSM are consistent with the expected range (122 ppb, Warneck, 2000; 84–127 ppb, Parrish et al., 1991; 110 ppb, Goldan et al., 1995; 120 ppb, Buhr et al., 1992; Doddridge et al., 1992; 96–112 ppb at Harvard Forest and 105 ppb from global model simulation, Li et al., 2004), while the results at MACA are considerably higher.

An adjusting parameter is applied to $NSR|_p$ to account for the fraction of SO_2 oxidized before the air masses arrived at the receptor site. The adjusting parameter is obtained by examining SO_4^{2-} and SO_2 data from a nearby Look Rock site (GRS420, 35°41′48″N, 83°36′35″W) of the Clean Air Status and Trends Network (CASTNet) jointly operated by the US EPA and NPS. Although the two sites are close, a spatial uniformity assumption that the ratio of $[SO_4^{2-}]$ to SO_2 is conserved within a short distance has to be made to extend the ratio measured at GRS420 to that at GRSM. The adjusting parameters for sulfur dioxide are 1.07, 1.14, 1.05, 1.03, and 1.07 for spring, summer, fall, winter, and overall data at GRSM, Cove Mountain, respectively. It should be pointed out that the value might be underestimated since a certain portion of sulfate may have been removed by dry and/or wet deposition processes before the air masses arrives at the site. Similar adjusting parameter data is not available for MACA due to the lack of sulfur measurements at or close to the monitoring site.

2.3. Influence areas based on trajectory-cluster analysis

The origin of air masses approaching a receptor site can be investigated by the combination of cluster analysis (Dorling et al., 1992) of hybrid single-particle lagrangian integrated trajectories (HY-SPLIT) model output (Draxler, 1997) and emission source categorization based on the EPA emission inventory (EPA, 2001). Cluster analysis is frequently employed in air pollution studies to address pollutant source origin. For instance, Slanina et al. (1983) and Pio et al. (1991) succeeded in identifying continental, maritime, and anthropogenic source regimes of pollutants based on cluster analysis. This method aims to maximize intergroup variance and to minimize intragroup variance. The algorithm chosen in this study is the one proposed by Dorling (1992). Briefly, endpoints of each trajectory are taken as input to the clustering algorithm. The first step chooses a large number of seed trajectories that cover the spread of real trajectories used in the analysis. All other trajectories are assigned to the seeds that can achieve minimum root mean square deviation (RMSD). The seed or average trajectory of each cluster is then recalculated from its members continuously until all trajectories are correctly assigned. After that, the number of clusters is reduced by merging the two closest clusters. The procedure repeats to find the RMSD for each cluster number and plot a graph of RMSD against the number of clusters. A sudden drop in RMSD as the number of clusters decreases is interpreted as the merging of clusters of trajectories that are significantly different in terms of the wind directions and speeds associated with the air masses.

The HYSPLIT-4 model was chosen to calculate air mass trajectories for cluster analysis. The actual operation routines are explained by Draxler (1997). Back trajectories were initialized at 1:00 PM local time and 500 m above the ground level. The selection of initial elevation in the back trajectory analysis has been the subject of considerable debate, particularly in regard to mountain-top sites such as GRSM. However, the uncertainty tends to be small when a large number of trajectories are averaged (Brankov et al., 1998). The 3-D motion is obtained using the nested grid model (NGM) for both horizontal and vertical air mass streams before April 1997. Results of data sets after April 1997 were obtained using 3-D hourly output from the Eta Data Assimilation System (EDAS). An optimum cluster number (Dorling, 1992) can be obtained by plotting the percentage change in the total RMSD (TRMSD) with respect to decreasing cluster numbers. Seven clusters were therefore retained as best describing significantly different forms of airflow to GRSM during the period. For reference, clusters were named according to their general direction: N, NE, S, etc. The cluster that stays closest to the receptor site is named C (close) because the speed of air parcels has influence on the level of pollutants.

2.4. Budget analysis using MAQSIP model

A comprehensive 3-D Eulerian grid model called Multiscale Air Quality SImulation Platform (MAQSIP) (Odman and Ingram, 1996) was used to study air quality in the southeast United State national parks. One of MAQSIP's attributes is a truly modular platform where physical/chemical processes are cast into modules following the time-splitting approach. Each process module operates on a common concentration field,

making it possible to conduct process budget analysis for each modeled specie (Kang et al., 2003). The detailed model setup, modeling domain, and time period are described by Kang et al. (2003). In this study, we analyze process budgets based on the model base scenario for modeled nitrogen species using the same technique that is described in Kang et al. (2003) for VOC species and O_3.

3. Results and discussion

3.1. Source apportionment of nitrogen oxides

Both methods discussed in Section 2.2 were employed to quantify the relative contribution of point sources to total nitrogen oxides emissions. Fig. 1 presents diurnal variations of point source contributions to total NO_y at

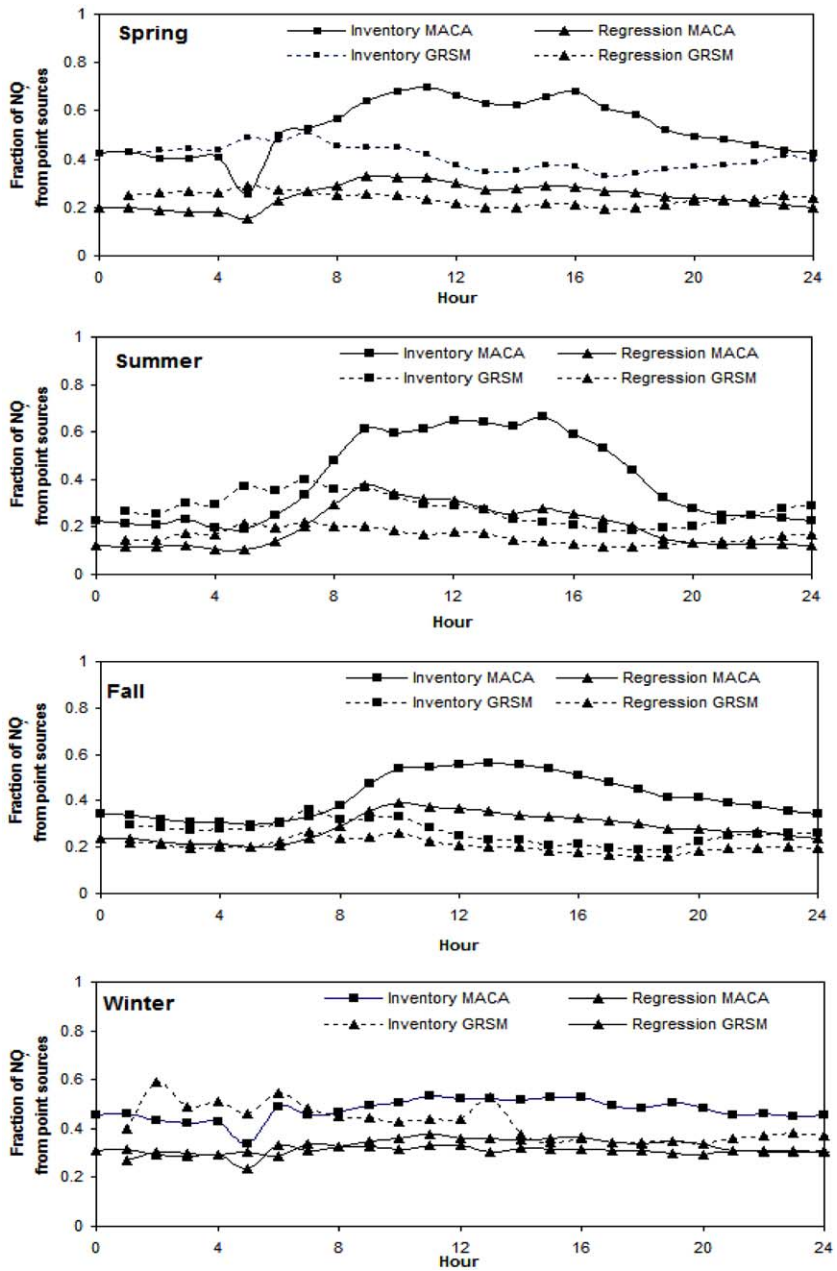

Fig. 1. Comparison of results from regression analysis and emission inventory analysis at the Great Smoky Mountain (GRSM) and Mammoth Cave (MACA) National Parks from 1995 to 1998.

GRSM and MACA for each season from 1995 to 1998. Results from both regression analysis and emission-inventory analysis reveal regular diurnal patterns at GRSM, which display weak maxima in early morning between 0500 and 0800 EST and minima in late afternoon between 1600 and 1800 EST during most of the year. In winter, however, irregular or no diurnal patterns are evident by this analysis. Results also reveal that CO and SO_2 do not display significant diurnal variation in winter, but do in other seasons (Tong et al., submitted manuscript, 2004). For MACA, Fig. 1 shows much stronger diurnal patterns for point source contributions to total NO_y in all seasons except winter. A larger influence by point sources is shown at MACA by higher fraction of contribution from point sources to NO_y and the broader daytime maximum. The calculated fractions from emission inventory analysis are higher than those from regression analysis for all seasons. In contrast to GRSM where the peak contribution from point sources is shortly after sunrise, at MACA the maximum is during midday (10–15 EST) and a minimum occurs before sunrise. Such diurnal trends can be largely explained by the activity of planet boundary layer (PBL). A stable nighttime boundary layer (NBL) forms over MACA that prevents air masses with a higher level of SO_2 from reaching the surface at night, while the lower NBL height and higher relative humidity hastens SO_2 removal level by dry deposition (Finkelstein et al., 2000) and heterogeneous chemistry (Jacob, 2000). Breakup of the nocturnal boundary layer above MACA triggered by sunrise allows air masses with transported SO_2 to mix downward to the surface during daytime.

Figs. 2 and 3 show a broader perspective of the diurnal and seasonal variations of the fraction of NO_y from point sources at GRSM and MACA. Contributions of point sources are calculated using the parameters presented in Tables 1 and 2, i.e., parameters derived from regression analysis of measurement data from GRSM and MACA. The episodic characteristics of the variations is much more apparent from these figures than as indicated by the diurnal plots. There is a seasonal difference in the portion of NO_y emissions from point sources at the two sites. The portion is generally higher during winter and spring, and lower during summer and fall at both sites. MACA has more frequent episodes that generally last longer than those at GRSM. Variations of the fraction would be expected to depend on both mobile and point source emissions, photochemistry during transport, and deposition processes. Point sources predominate in wintertime when SO_2 has a longer lifetime than in summertime, which may alter the concentrations of SO_2 relative to NO_y and CO and the correlations between these species observed at the receptor site. Visual inspection of high point source periods in Figs. 2 and 3 shows a lack of strong diurnal

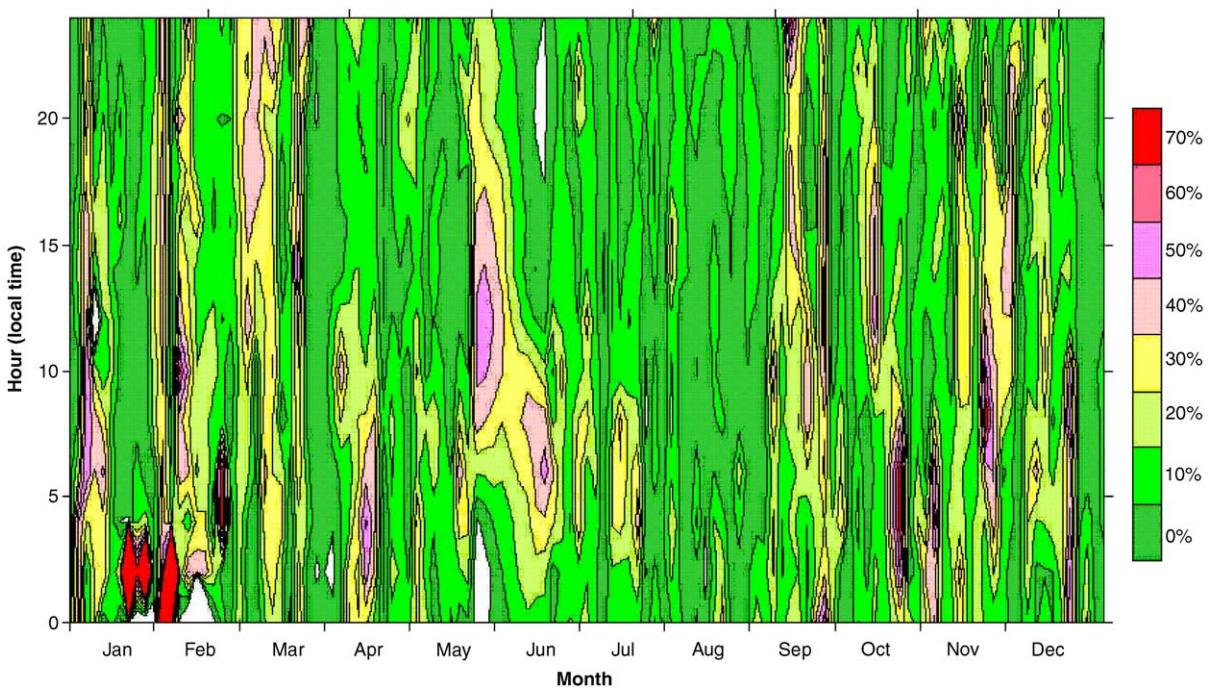

Fig. 2. Diurnal and seasonal variation of fraction from point sources to total reactive nitrogen (NO_y) at the Great Smoky Mountain (GRSM) National Park, TN/NC, 1996.

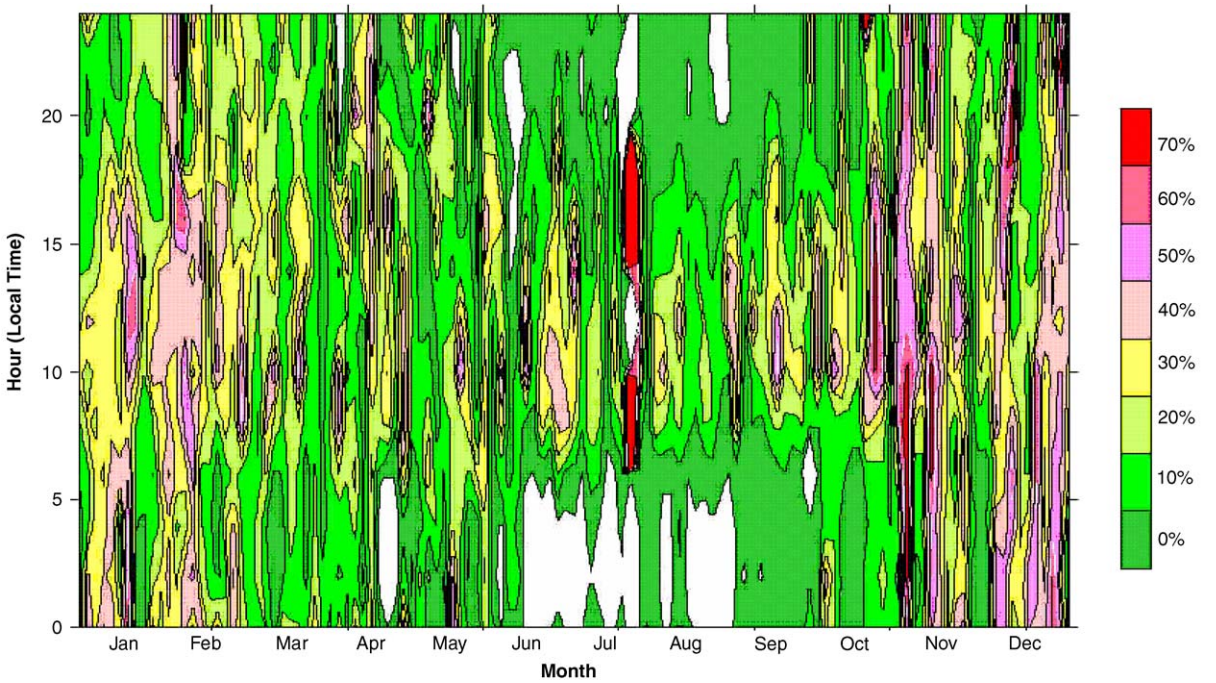

Fig. 3. Diurnal and seasonal variation of fraction from point sources to total reactive nitrogen (NO_y) at the Mammoth Cave (MACA) National Park, KY, 1996.

variation at GRSM, whereas MACA has a diurnal variation in summer that broadens to overnight periods in fall and winter.

Figs. 2 and 3 also illustrate that the relative contribution from point sources to NO_y is higher at MACA than at GRSM. Direct measurements show that total NO_y is higher at MACA (annual average of 6.9 ppbv at MACA vs. 4.0 ppbv at GRSM, respectively, Tong et al., submitted manuscript, 2004). Point sources around Mammoth Cave national park may play a more important role in the evolution of nitrogen oxides there. The higher fraction of NO_y from point sources and the higher concentrations of NO_y seen in the daytime maximum of the diurnal pattern at MACA corresponds to the most photochemically active period when ozone concentrations are highest at MACA. Occasionally in the middle of summer, point sources provide up to 70% of total NO_y, which is widely considered as the limiting factor of photochemical O_3 production in the rural southeast areas (Jacob et al., 1995; SOS, 2001; Kang et al., 2003). Table 3 shows summaries of point source contributions to total NO_y for each season at GRSM and MACA, as well as results from previous studies for other locations in the eastern United States (Stehr et al., 2000). Both analyses show lower fractions of NO_y from point sources in summer and fall, and higher in winter and spring. Point sources contribute 16–22% and 30–38% to total reactive nitrogen oxides in summer and winter at GRSM, and 21–40% and 33–47% at MACA. Generally, regression analysis provides lower fraction values than emission-inventory analysis. A similar pattern is reported in other case studies for three northeast US sites (Stehr et al., 2000). Both techniques are based on measured SO_2 and CO concentrations at the receptor site to estimate point source contribution. However, emission-inventory analysis is also dependent on the estimated background CO and the adjustment parameter for SO_2. An overestimate of background CO concentration or an underestimate of the SO_2 parameter may result in a lower mobile source emission contribution and, therefore, overestimate the contribution from point source emissions to total NO_y. The ratios adopted in the emission-inventory analysis represent those for freshly emitted air masses and may not reflect the influence of oxidization, deposition, and other removal processes, especially for a remote site, unless an accurate adjustment parameter is available. As a result, regression analysis may provide a better estimate for a remote site. It should be pointed out that regression analysis is also subject to uncertainties introduced by certain events during long-range transport (Stehr et al., 2000). A possible refinement is to adopt the reduced major axis regression, rather than standard linear regression used here (Ayers, 2001).

Table 3
Estimation of contribution of point sources to total NO_y emission at Eastern US sites

Sites	Periods	Regression analysis (%)	Emission inventory analysis (%)	Emission inventory analysis[a] (%)
GRSM, TN[b]	Spring (MAM)	23	34	35
	Summer (JJA)	16	22	24
	Fall (SON)	20	21	22
	Winter (DSF)	30	38	39
	All data	23	26	27
SHEN, VA[c]	September–December	29±5	30±8	34±8
MACA, KY[b]	Spring (MAM)	25	53	—
	Summer (JJA)	21	40	—
	Fall (SON)	29	42	—
	Winter (DSF)	33	47	—
	All data	27	45	—
Wye, MD[c]	September–December	11±5	16±4	20±5
Arendiville, PE[c]	June–September	21±3	26±6	32±8

[a]Adjusted by sulfur oxidization factor.
[b]95% confidence interval on the mean.
[c]Stehr et al., 2000.

3.2. Influence areas based on trajectory-cluster analysis

Individual trajectories in 1996 were calculated using the HSPLIT-4 model for those days when simultaneous measurements of O_3 and NO_y were available at GRSM. The whole trajectory set was then clustered into seven groups using the clustering algorithm discussed earlier. A seed trajectory—a trajectory that can minimize the average RMSD for all other trajectories within a cluster—was selected out of each cluster. Fig. 4(a) illustrates the chosen seed trajectories from each cluster. Each seed trajectory is labeled with the direction best describing the relative position of its origin and general path to the receptor site. The number in parentheses shows the percentage of trajectories assigned to a particular cluster. Emission density of NO_y, taken from the EPA county-based emission inventory (EPA, 2001), is displayed as the background in Fig. 4(a) to provide a visual indicator of regional emission levels that might be loaded into those air parcels following a cluster trajectory. Fig. 4(a) shows that air masses from west (W, 20%) and southwest (SW, 17%) sweep GRSM most frequently, while pollutants transported from the eastern half (i.e., Eastern, Northeast, or Southeast) have limited influence (<10%) on air quality in the Great Smoky Mountain national park. Air masses originated from or traveling through the Ohio Valley region (i.e., far north (FN) or close north (CN)), which was marked as high level of NO_y emissions, account for more than one quarter of the total trajectory number. Examining pollutants associated with these individual clusters can provide further information on the magnitude of influence from the corresponding source areas.

The average O_3 and NO_y concentrations associated with each cluster are presented in Fig. 4(b). The highest O_3 concentrations are associated with trajectories from the CN cluster (55.4 ppbv) and FN cluster (52.6 ppbv). Both CN and FN trajectories originated from the Ohio Valley region or adjacent areas. Air masses in SW cluster also carry high levels of ozone (54.5 ppbv) to GRSM. Trajectories in the SW cluster are generally traced back to the coastal region of the Gulf of Mexico, where high levels of nitrogen oxides emissions exist. There are two possible mechanisms responsible for high ozone concentration in SW cluster. One is that clean marine air masses load high ozone content when traveling through certain regions, in which case either C (Close) or W (Western) will contain higher levels of ozone than SW since those air masses have to go through either of these regions before reaching GRSM. However, Fig. 4(b) reveals no evidence to support this hypothesis. The other one would be that air masses load high ozone content (i.e., O_3 precursors, NO_x and VOCs, as well as O_3) from polluted coastal regions, and photochemistry produces more O_3 during the transit to GRSM. Of course, other arguments may arise since ozone presence is a mixture of remote transport, local production, and removal processes. However, as indicated by the process budget analysis using a 3-D chemistry and transport model, transport (about 80%) is the dominant process in O_3 concentrations at GRSM. In combination with the results of trajectory-cluster

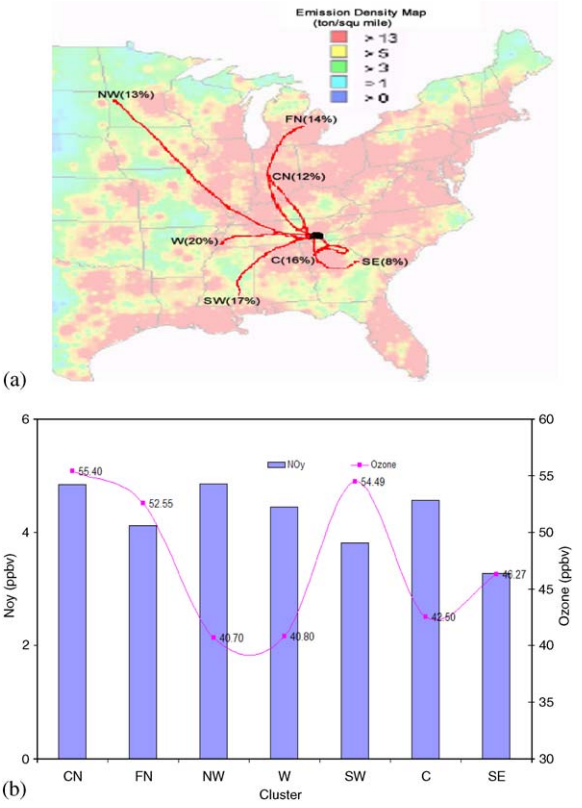

Fig. 4. (a) Average trajectory of each cluster of air masses approaching the Great Smoky Mountain (GRSM) National Park, TN/NC. Each average trajectory is labeled with the relative position of its origin to the receptor site. The number in the parenthesis shows the percent of the trajectories assigned to a particular cluster. The background is emission density of NO_y taken from EPA (1999). (b) Average NO_y and O_3 associated with each cluster displayed in (a).

analysis, we deduce that (1) the polluted regions hundreds of miles away, such as the Ohio Valley and Gulf of Mexico, may be linked to air quality at GRSM; (2) a 48-h running period can well address emission origin, in other words, air masses of concern will have a photochemical age of 2–3 days, consistent with the fact that mean atmospheric residence time for gaseous nitrogen oxides is in 1–4 days (Seinfeld and Pandis, 1998, p. 74).

The relationship between O_3 and NO_y concentrations associated with each individual trajectory cluster was investigated (Fig. 4b). O_3 concentrations in the NW, W, and C clusters were low, while NO_y concentrations in those clusters were high. This discrepancy can be attributed to either VOC-limited ozone production or to the fact that nitrogen oxides have not fulfilled their potential to produce more ozone (Kim et al., 1994; Jacob et al., 1995; Ryerson et al., 2001). Examination of NO_y production efficient can provide evidence to judge this argument. Scatter plots of O_3 against NO_y (not shown here) reveal lower slopes for W and C clusters, compared to other clusters, but not for NW cluster. It turns out that seasonality plays an important role in determining the ratio of O_3 to NO_y associated with a cluster. A cluster containing trajectories predominately of cold seasons is likely associated with a lower $[O_3]$ to $[NO_y]$ ratio than that of warm seasons.

3.3. Process budget analysis of nitrogen oxides by MAQSIP

Six processes—chemistry (CHEM), horizontal advection (HADV), vertical advection (VADV), vertical mixing (VDIF), emissions (EMIS), and dry deposition (DDEP)—have a significant effect on budgets of nitrogen compounds. Fig. 5 shows the mean contribution rates over the entire modeling period (1000–1700 EST) of each process for NO_x and NO_z ($NO_z = NO_y - NO_x$), respectively, in the grid cells representing the national parks. The reason that NO_z instead of NO_y is analyzed is that NO_z is primarily the end product of NO_x and is considered as a good indicator of O_3 production. Therefore, NO_z may offer more information about the contribution of nitrogen oxides to O_3 production. Even though the major contributions to NO_x production at the two locations come from horizontal advection (58–62%) and local emissions (38–42%), and the primary removal process for NO_x is local chemistry (92–95%), the magnitude of each process at MACA is more than three times larger than that at GRSM, which matches the observed results (1.2–4.8 times, Tong et al., submitted manuscript, 2004). In the NO_z side, however, 84% of NO_z is the result of local chemistry at MACA, which accounts only for 32% at GRSM; the rest comes from transport. About half of NO_z is removed by dry deposition at GRSM, while the rate is 87% at MACA. The remaining NO_z at MACA is removed through transport. Also note that unlike NO_x, the combined magnitude of process contributions to NO_z is similar across the two locations.

If we compare the process budgets of NO_z with that of O_3 (Fig. 5, recreated from Kang et al., 2003), the similarity among the locations as well as the contributions of each individual process at each location is apparent, especially on the positive side. For instance, chemistry contributions of 32% and 84% to NO_z correspond to 26% and 80% to O_3 at GRSM and MACA, respectively. The other primary contributions to the accumulation of NO_z and O_3 are from horizontal advection at GRSM and vertical advection at MACA. The difference for the transport contributions to NO_z and O_3 at MACA is that both horizontal and vertical advection processes contribute to NO_z, but only vertical advection process contributes to O_3. On the removal side, dry deposition is the primary process to remove

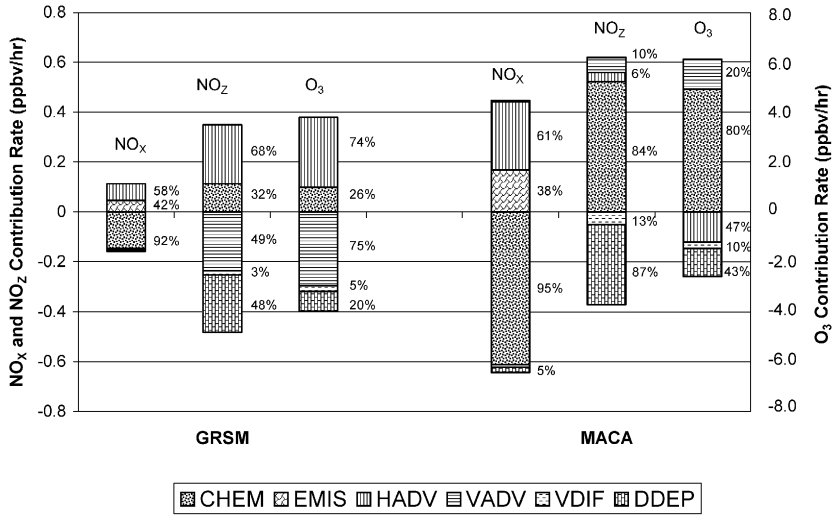

Fig. 5. Process budget analysis of NO_x, NO_z, and O_3 using MAQSIP in the chosen domain during the 1995 summer time.

NO_z at all three locations, but it is only responsible for 20–43% of O_3 removal. Transport processes (either horizontal or vertical) are responsible for removal of the remaining NO_z and O_3, with a more important role in removing O_3 than removing NO_z. Nevertheless, the similarity between NO_z and O_3 process budgets further demonstrates that NO_z can be used as evidence of close association between nitrogen oxides and effective O_3 production at these rural locations.

4. Conclusion and implications

This study has focused on both observation-based and modeling analyses in elucidating source attribution, influence area, and process budget of reactive nitrogen oxides at two rural national parks in the southeast United States. A regression analysis indicates mobile sources are the predominant source of NO_y at both sites while point sources contributed approximately 23% and 27% of total NO_y at GRSM and MACA, respectively. Another technique, emission-inventory analysis, provides that a minimum of 26% for GRSM and 45% for MACA of total NO_y can be attributed to point source emissions on the basis of continuous measurements of CO and SO_2. The discrepancy between the two methods is largely a result of uncertainty in the emission inventory and in determination factors such as background CO and SO_2 adjustment parameter. A more sophisticated approach, comprehensive 3-D air quality modeling, might be used as an alternative to address this source apportionment problem. Nevertheless, we demonstrate that a minimum of one quarter of reactive nitrogen oxides at the two parks are emitted by point sources located within air mass transport distance of the receptor sites.

These two rural parks have high levels of ambient O_3 in excess of the national standard of 0.08 ppm for an 8-h average several times each year and are characterized by strong biogenic VOC sources (Ryerson et al., 2001; Kang et al., 2001, 2003). Computer modeling has suggested that both sites are NO_x-limited in the formation of O_3. From a source contribution standpoint, both locations get their NO_y from predominately mobiles sources, yet there are significant differences in how the NO_y affects the observed ozone. MACA has a much larger proportion of O_3 and NO_y from local photochemical production; the NO_y is less aged (less oxidized) and fresh emissions play a larger role in the chemical processing. Point sources are much more likely to be episodic and during daytime hours at Mammoth Cave, suggesting that plumes from single or multiple sources, if along the same trajectory, are responsible for the episodes. GRSM also has NO_y predominately from mobile sources and has episodic point source events, but these are less frequent and less likely to happen just at midday. The NO_y is more aged (more oxidized) and both NO_y and O_3 at GRSM are predominately transported by horizontal advection (about 70%).

Trajectory-cluster analysis shows that air masses at GRSM are most often from the western and southwest, while pollutants transported from eastern half (i.e., eastern, northeast, or southeast) have limited influence ($< 10\%$) on air quality in the Great Smoky Mountains national park. Air masses originated from or traveling through the Ohio Valley region account for more than one quarter of the total trajectory number. Examination of pollutants associated with individual

clusters reveals that the highest O_3 concentrations are in air masses from the north and southwest directions, which can be traced back to the Ohio Valley region and to the high-emission coastal regions along the Gulf of Mexico. Caution must be exercised, however, that results of this study be limited to the time period during which trajectories were calculated. We have chosen only those trajectories for days when simultaneous O_3 and NO_y measurements were available.

The processes responsible for the production and removal of reactive nitrogen oxides were investigated using the MAQSIP model. The contribution associated with local chemical transformations for NO_z and O_3, based on process budget analysis, is 32% and 84% for NO_z, and 26% and 80% for O_3 at GRSM and MACA, respectively. The similarity between NO_z and O_3 process budgets serves as further evidence of close association between nitrogen oxides and effective O_3 production at these rural locations. One may note that this modeling study is limited to summertime when biogenic emission is most active. High ozone events in southeast national parks, however, have been frequently observed in seasons other than summer, during which ozone photochemistry may be characterized by non-NO_x-limiting conditions (Kleinman, 1991; Jacob et al., 1995; Sillman and He, 2002). One of the recent findings by the NARSTO (2002) suggests that this may be an over simplification since VOC or NO_x limitation is not uniquely defined by location or emissions. Further efforts are needed to address the seasonal characteristics of high ozone episodes and ozone precursors that contribute to shape air quality in the rural southeast areas.

Acknowledgements

This research was funded by the National Park Service, Air Resources Division, cooperative agreement #4000-7-9003. The authors thank Dr. Rohit Mathur in Carolina Environmental Program, University of North Carolina at Chapel Hill for his help in the modeling and data processing, and Binyu Wang at North Carolina State University for her assistance in statistical analysis. Thanks to Bob Carson, Scott Berenyi, and Jim Renfro (NPS), and to Ken Olszyna (TVA) for their efforts in collecting the data.

References

Aneja, V.P., Businger, S., Li, Z., Claiborn, C.S., Murthy, A., 1991. Ozone climatology at high elevations in the southern Appalachians. Journal of Geophysical Research 96, 1007–1021.

Ayers, G.P., 2001. Comment on regression analysis of air quality data. Atmospheric Enviroment 35, 2423–2425.

Brankov, E., Rao, S.T., Porter, P.S., 1998. A trajectory-clustering-correlation methodology for examining the long-range transport of air pollutions. Atmospheric Environment 32 (9), 1525–1534.

Buhr, M.P., Trainer, M., Parrish, D.D., Sievers, R.E., Fehsenfeld, F.C., 1992. Assessment of pollutant emission inventories by principal component analysis of ambient air measurements. Geophysical Research Letters 19, 1009–1012.

Chameides, W.L., Saylor, R.D., Cowling, E.B., 1998. Ozone pollution in the rural United States and the new NAAQS. Science 276, 916.

Doddridge, B.G., Dickerson, R.R., Wardell, R.G., Civerolo, K.L., Nunnermacker, L.J., 1992. Trace gas concentrations and meteorology in rural Virginia 2: reactive nitrogen compounds. Journal of Geophysical Research 97, 20631–20646.

Dorling, S.T., David, T.D., Pierce, C.E., 1992. Cluster analysis: a technique for estimating the synoptic meteorological controls on air and precipitation chemistry—method and applications. Atmospheric Environment 26A, 2575–2581.

Draxler, R.R., 1997. Description of the HYSPLIT_4 modeling system. National Oceanic and Atmospheric Administration technical Memorandum ERL ARL-224.

Environmental Protection Agency, 1997. National air pollutant emission trends, 1900–1996. EPA-454/R-97-011, Washington, DC.

Environmental Protection Agency, 2001. National air pollutant emission trends, 1999, EPA-454/R-01-004, Washington, DC.

Finkelstein, P.L., Ellestad, T.G., Clarke, J.F., Meyers, T.P., Schwede, D.B., Hebert, E.O., Neal, J.A., 2000. Ozone and sulfur dioxide dry deposition to forests: observations and model evaluation. Journal of Geophysical Research 105, 15,365–15,377.

Goldan, P.D., Trainer, M., Kuster, W.C., Parrish, D.D., Carpenter, J., Roberts, J.M., Yee, J.E., Fehsenfeld, F.C., 1995. Measurements of hydrocarbons, oxygenated hydrocarbons, carbon monoxide, and nitrogen oxides in an urban basin in Colorado: Implications for emissions inventories. Journal of Geophysical Research 100, 22,771–22,783.

Jacob, D.J., 2000. Heterogeneous chemistry and tropospheric ozone. Atmospheric Environment 34, 2131–2159.

Jacob, D.J., Horowitz, L.W., Munger, J.W., Heikes, B.G., Dickerson, R.R., Artz, R.S., Keene, W.C., 1995. Seasonal transition from NO_x- to hydrocarbon-limited conditions for ozone production over the eastern United States in September. Journal of Geophysical Research 100, 9315–9324.

Kang, D., Aneja, V.P., Zika, R.G., Farmer, C., Ray, J., 2001. Nonmethane hydrocarbons in the rural southeast United States national parks. Journal of Geophysical Research 106, 3133–3155.

Kang, D., Aneja, V.P., Mathur, R., Ray, J., 2003. Nonmethane hydrocarbons and ozone in the rural southeast United States national parks: a model sensitivity analysis and its comparison with measurement. Journal of Geophysical Research 108 (D10), 4604.

Li, Q., Jacob, D. J., Munger, J.W., Yantosca, R.M., Parrish, D.D., 2004. Export of NO_y from the North American

boundary layer: reconciling aircraft observations and global model budget. Journal of Geophysical Research 109.

Lippmann, M., 1992. Environmental Toxicants: Human Exposures and Their Health Effects. Van Nostran Raeinhold, New York.

NARSTO, 2002. An Assessment Of Tropospheric Ozone Pollution: A North American Perspective. pp. 3–11 (Chapter 3) (available from http://narsto.owt.com/Narsto/assess.doc.html).

National Research Council (NRC), 1991. In: Seinfeld, J.H. (Chair), Rethinking the Ozone Problem in Urban and Regional Air Pollution. National Academic Press, Washington, DC, 4889pp.

Odman, T., Ingram, C.L., 1996. Multiscale air quality simulation platform (MAQSIP): source code documentation and validation. MCNC Technical Report, ENV-96TR002-v1.0.

Olszyna, K.J., William, J.P., James, F.M., 1998. Air chemistry during the 1995 SOS/Nashville intensive determined from level 2 network. Journal of Geophysical Research 103, 31,143–31,153.

Parrish, D.D., Trainer, M., Buhr, M.P., Watkins, B.A., Fehsenfeld, F.C., 1991. Carbon monoxide concentration and their relation to concentrations of total reactive oxidized nitrogen at two rural US sites. Journal of Geophysical Research 96, 9309–9320.

Pio, C.A., Santos, I.M., Anacleto, T.D., Nunes, T.V., 1991. Particulate and gaseous air pollutant levels at the Portuguese west coast. Atmospheric Environment 25A, 669–680.

Ryerson, T.B., et al., 2001. Observations of ozone formation in power plant plumes and implications for ozone control strategies. Science 292,27.

Saeger, M., et al., 1989. The 1995 NAPAP emissions inventory (version 2): development of the annual data and modelers tapes. Rep. EPA-600/7-89-12a, EPA, Washington, DC.

Seinfeld, J.H., Pandis, S.N., 1998. Atmospheric Chemistry and Physics. from Air Pollution to Climate Change. Wiley, New York 74pp.

Slanina, J., Baard, J.H., Zijp, W.L., 1983. Tracing the sources of chemical composition of precipitation by cluster analysis. Water, Air & Soil Pollution 20, 41–45.

Sillman, S., He, D., 2002. Some theoretical results concerning O3-NO_x-VOC chemistry and NO_x-VOC indicators. Journal of Geophysical Research 107 (D22), 4659.

SOS Report, 2001. The state of the southern oxidants study-2: policy relevant findings in ozone and $PM_{2.5}$ pollution research 1994–2000. North Carolina State University, Raleigh, North Carolina, 27695.

Stehr, J.W., Dickerson, R.R., Hollock-Waters, K.A., Doddridge, B.G., Kirk, D., 2000. Observations of NO_y, CO, and SO_2 and the origin of reactive nitrogen in the eastern United States. Journal of Geophysical Research 105, 3553–3563.

Tennessee Valley Authority (TVA), 1995. SOS Nashville/Middle Tennessee Ozone Study, vol. 2, Level 2 operations manual, Environ. Res. Cent., Muscle Shoals, Ala.

Warneck, P., 2000. Chemistry of the Natural Atmosphere. Academic Press, New York.